Propagation of Complex Laser Pulses in Optically Dense Media

M. R. Fetterman, J. C. Davis, D. Goswami, W. Yang, and W. S. Warren
Princeton University Center for Ultrafast Laser Applications, Princeton University, Princeton, New Jersey 08544
(Received 21 December 1998)

Ultrafast laser pulses with complex envelopes (amplitude and frequency modulated) are used to excite an optically dense column of rubidium vapor. Pulse reshaping, stimulated emission dynamics, and residual electronic excitation in the Rb vapor are all shown to depend strongly on the laser pulse shape. Pulses that produce adiabatic passage in the optically thin limit exhibit more complex behavior in optically thick samples, including an unexpected dependence on the sign of the frequency sweep. Numerical solutions of the Maxwell-Bloch equations are shown to account for our results. [S0031-9007(99)09123-1]

PACS numbers: 42.62.Fi, 32.70.Jz, 42.65.Re

In recent years, it has become apparent that optical pulse shaping alters excitation dynamics in atomic and molecular systems [1,2]. Some similar effects have been known for decades both in nuclear magnetic resonance and in magnetic resonance imaging, where the technology to tailor radiofrequency pulses has been used routinely for several decades [3]. For the case of laser-matter interactions, however, the combination of optical density and wave packet dynamics also leads to completely new physical phenomena, which are just beginning to be explored as the technology for optical pulse shaping matures [4].

Here, we use pulse shaping technology to make complex phase- and amplitude-modulated picosecond laser pulses with sufficient intensity to leave the linear-response regimes, and we apply such pulses to optically dense samples of Rb vapor. In the absence of optical density effects, the pulse shapes we apply [field envelope proportional to $\mathrm{sech}(\alpha t)^{(1+\mu i)}$, or equivalently a sech pulse envelope with a tanh frequency sweep] are predicted to give complete, bandwidth limited inversion [5]. For an optically dense sample, however, we report different dynamics that depend upon the input pulse shape. These results may be of practical importance in preparing spin-polarized noble gases, the only reagents commercially prepared today using laser systems [6].

The coupled Maxwell-Bloch (MB) equations describe both the evolution of a material system and the reshaping of the laser pulses as they propagate through an optically dense medium [7]. This system of equations combines Maxwell's wave equation with Bloch's quantum-mechanical description of the field-matter interaction and are written

$$\frac{\partial E(\vec{\zeta},\tau)}{\partial \tau} = \frac{i}{g(0)} \int_{-\infty}^{\infty} g(\Delta') p(\vec{\zeta},\tau,\Delta')\, d\Delta', \quad (1)$$

$$\frac{\partial p(\vec{\zeta},\tau,\Delta')}{\partial \tau} = \left[-\frac{1}{T_2} + i2\pi\Delta \right] p(\vec{\zeta},\tau,\Delta') - iE(\vec{\zeta},\tau) w(\vec{\zeta},\tau,\Delta'), \quad (2)$$

$$\frac{\partial w(\vec{\zeta},\tau,\Delta')}{\partial \tau} = -\mathrm{Im}[E(\vec{\zeta},\tau)\, p^*(\vec{\zeta},\tau,\Delta')] - \frac{wp^* - w_0}{T_1}. \quad (3)$$

Here, $E(\vec{\zeta},\tau)$ is the electric field, which is a function of three spatial coordinates, represented by the vector $\vec{\zeta}$, and of time, $g(\Delta)$ is the inhomogeneous line shape at resonance offset Δ, $p(\vec{\zeta},\tau,\Delta')$ is the polarization, T_2 and T_1 are the coherence and population lifetimes, respectively, and $w(\vec{\zeta},\tau,\Delta')$ is the population difference. We used recursive algorithms developed in [8,9] to solve the MB equations numerically.

The hyperbolic secant pulse with a hyperbolic tangent frequency sweep (sech) mentioned above is an analytical solution to the Bloch equations [5] and has received a great deal of attention [5,7,8] due to its success at inducing complete bandwidth limited inversions in material systems. This pulse may be written as a complex field envelope,

$$E(t) = \mathrm{sech}(\alpha t)^{(1+\mu i)}, \quad (4)$$

where α is related to the (amplitude) FWHM of the pulse ($\tau = \frac{2.6}{\alpha}$). For the case where $\mu = 0$, self-induced transparency is observed if the sech pulse has the correct area ($2n\pi$). When μ is nonzero, the instantaneous frequency of the pulses changes with time and the laser can induce adiabatic rapid passage (ARP) [3,7,10] in a two-level system.

Most treatments of laser pulse propagation in the literature focus upon laser pulses whose bandwidths are narrower than the inhomogeneous linewidth associated with the material systems ("narrow band limit") [8]. Thus, reshaping in the temporal domain has been stressed. Propagation of broad bandwidth Gaussian laser pulses through potassium vapor was recently shown [11], both experimentally and theoretically (by numerically solving "plane wave" Maxwell-Bloch equations), to reshape in a complex oscillatory manner.

 0031-9007/99/82(20)/3984(4)$15.00

An ultrafast laser pulse shaping system was used to generate the sech pulses described by Eq. (4). This system [12] features an acousto-optic modulator and is capable of shaping both the amplitude and phase of laser pulses. The output pulses of this amplified pulse shaper characteristically have energies of 200 μJ/pulse and minimum pulse lengths of 120 fs. The pulses were focused into a spot size of approximately 0.5 cm^2 at the Rb cell.

We also used the STRUT (spectrally and temporally resolved up-conversion technique [13]) to characterize the pulses. Like the FROG (frequency resolved optical gating [14]) and SPIDER (spectral phase interferometry for direct electric-field recovery) [15], the STRUT is a measurement technique that allows recovery of the phase and amplitude of laser pulses. The STRUT signal arises from sum-frequency generation between the shaped pulse and a narrow band reference (derived from spectrally filtering a piece of the pulse). The sum-frequency spectrum is measured (0.3 nm resolution) as a function of the reference pulse delay. The up-converted signal at the second harmonic crystal is given by

$$E_{\mathrm{up}}(\tau, \delta) \propto \int d\delta\, E_r(\delta') e^{i\delta'\tau} E_p(\delta - \delta'). \qquad (5)$$

From Eq. (5), along with some nonrestrictive assumptions, it can be shown that the full phase and amplitude information of $E(\omega)$ can be recovered [13].

The Gaussian pulses we used in these experiments (the unshaped pulses) typically had a FWHM of 6 nm and a temporal length of 150 fs. Shaped pulses, with $\alpha = 1.0 \times 10^{12}$ and $\mu = -8$ or $\mu = +8$ as in Eq. (4), denoted "sech$-$" and "sech$+$", respectively, were generated by our pulse shaping system. The sech$-$ pulses are frequency swept from longer to shorter (red to blue) wavelengths and the sech$+$ pulses are chirped from shorter to longer (blue to red) wavelengths. A typical spectrum of a sech$-$ pulse is shown in Fig. 1 (solid line). The dashed line spectrum depicts a weak sech$-$ pulse after passing through Rb vapor.

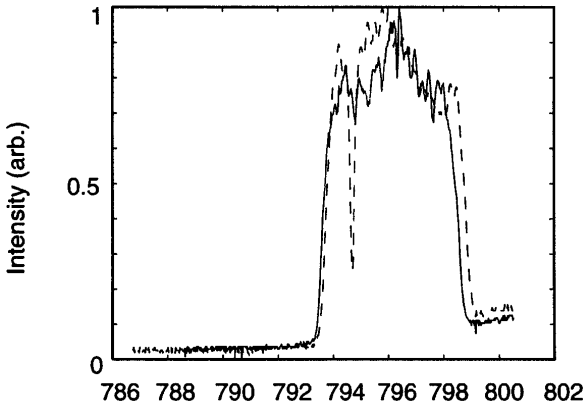

FIG. 1. Spectrum of a typical sech$-$ pulse as used in our experiments. The solid line shows the pulse without the cell, and the dashed line shows a weak pulse after propagating through the cell. Note that the dashed line and the solid line curves were taken on different days, so that they may appear slightly different.

In Fig. 2, a theoretical STRUT image of a sech$-$ pulse (a) is compared with an experimental STRUT trace (b) of the same pulse shape before propagating through Rb vapor. The tanh frequency sweep is clearly discernible in these traces. The tanh frequency sweep of the sech$+$ pulse is a reflection of that of the sech$-$ pulse (not shown). In contrast, the STRUT trace of a transform limited Gaussian is circular. Figure 2c is the STRUT trace of the sech$-$ pulse after propagation through the Rb cell (and is discussed in further detail below).

In this Letter, we focus upon the D_1 line of Rb (centered at 794.7 nm), which may be modeled as a two-level system (the two electronic transitions nearest the D_1 line, the $5S_{1/2} \rightarrow 5P_{3/2}$ and $5P_{3/2} \rightarrow 5D_{3/2}$ are, respectively, at 780.2 and 775.9 nm [16] and lie beyond the bandwidth of our pulses). Furthermore, the hyperfine splittings of the $5S_{1/2}$ and $5P_{1/2}$ levels are not resolvable due to pressure broadening.

We measured the spectra and the STRUT spectrograms of the laser pulses through the Rb cell and studied the excited state dynamics of the spectral features we observed via pump-probe experiments. The Rb cell was constructed with optical quality, alumina silicate glass, and was filled with helium to a backpressure of 200 Torr. We also measured similar spectra using a cell containing Rb and nitrogen (similar to those cells used for producing spin-polarized noble gases), which indicates that the effects shown here are not related to a Rb-helium van der Waals interaction. The Rb is in the solid state until it is heated to 100 °C, at which point significant vapor pressure forms. The cell was heated, typically to 150 °C, by wrapping electrical heating tape around it. The spectrometer was located approximately 3 m away from the cell. There were no lenses between the cell and the spectrometer.

We first analyzed the weak beam passing through the cell to determine the parameters of the atomic line shape. The He buffer gas in our Rb cell collisionally broadened the D_1 line to a FWHM of 0.6 THz, which gives a collisional dephasing time of $T_2 = 1.7$ ps. In this weak field limit, the optical density (OD $= \log_e \frac{I_0}{I}$) of the transition was found to be approximately 4.

In Fig. 3, we show the spectra of the three types of laser pulses after passing through the Rb cell. These pulses are all intense enough [on the order of $\theta =$ multiple$(2-7)\pi$ pulses] to induce nonlinear effects. In Fig. 3a, the intense Gaussian pulse (solid line) is depicted after having passed through the cell. The dip on the left side of this spectrum appears to be an absorption feature, and the peak on the right an emission feature. The theoretically modeled spectrum (dashed), calculated using the paraxial MB equations, also illustrates the same dynamics. In these calculations, OD $= 4$, and the on-axis pulse area is 1.2π.

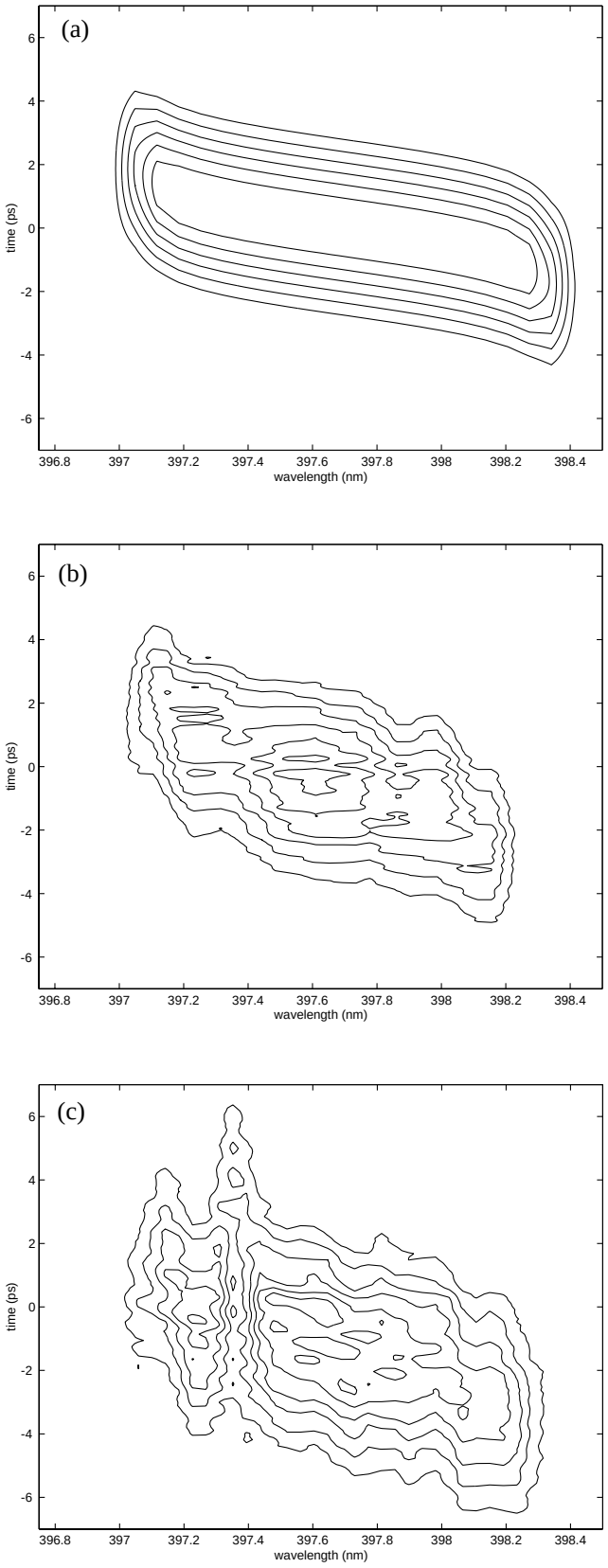

FIG. 2. STRUT traces of (a) theoretical sech−, (b) experimental sech− before the Rb cell, and (c) experimental sech− pulses after the Rb cell. The contour lines represent linear steps in intensity.

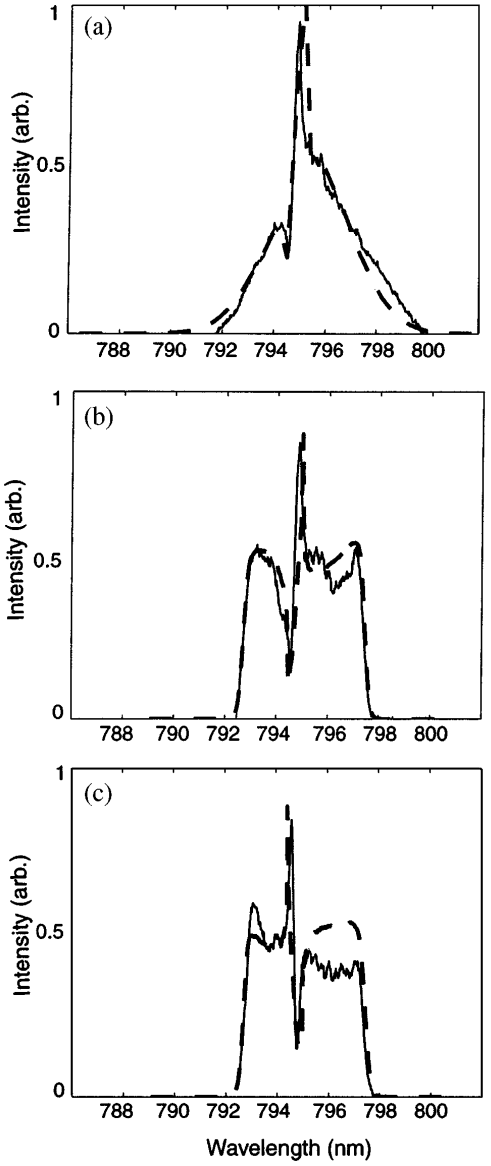

FIG. 3. Spectra of intense laser pulses after propagation through Rb vapor. (a) is an initially unchirped Gaussian, (b) is a sech+ pulse, and (c) is a sech− pulse. Solid lines represent experimental data and dashed lines are theoretical fits.

In Fig. 3b (solid line) the absorption spectrum of the sech+ pulse is shown. Here, once again, the dip and the peak are visible in the same sequence as in Fig. 3a. The dashed line in Fig. 3b represents the theoretical fit (OD $= 4$, $\mu = +8$, and the pulse area is $4 \times A_\pi$, where A_π is the area of a π pulse on axis when $\mu = 0$). Finally, in Fig. 3c we show the absorption profile of the sech− pulse. It can be seen that in this case the dip and the peak are now reversed. The theoretical fit (OD $= 4$, $\mu = -8$, and the pulse area is $4 \times A_\pi$) for Fig. 3c shows the same dip and peak order as that observed experimentally. The dip and peak features are also evident in the STRUT trace of Fig. 2c on the left-hand side. The dip is manifest as

a break in the intensity contours of the STRUT trace, whereas the peak contours trail the rest of the pulse.

The experimental data are consistent with our numerical simulations, which indicates that all of the observed phenomena are included in the Maxwell-Bloch equations. Similar experimental features were observed in [11], where an analysis was put forth to explain these results qualitatively. A dispersive feature (dip/peak) arises for off-resonance pulses in the thin sample limit when the flip angle $\sim\pi$. This feature results from the interaction between the laser radiation and the induced dipole field and flips orientation depending upon the sign of the detuning. Thus, for the frequency-modulated pulses, the orientation of the dip/peak feature depends upon the direction of the sweep (and thus the direction from which resonance is approached). In the high OD limit, on the other hand, the interactions between the laser field and medium are more complex, and the features oscillate in a complicated manner (that is, however, predictable via MB simulations). For the unchirped Gaussian pulses, the orientation of the dip/peak feature depends upon the detuning of the center frequency of the pulse from the transition frequency.

In order to characterize the emission feature, we looked at its polarization, which we found to be different from that of the input pulses alone. We also found that the laser beam self-focuses as it propagates through Rb. Finally, we implemented a pump-probe experiment that indicated that the sech$-$ pulse is more effective at exciting population in Rb than the other pulse shapes. Specifically, the gain measured for the sech$-$ probe pulses was 15, and was 7.5 and 2.5 times larger than the gain measured for the sech$+$ and Gaussian pulses, respectively. Thus, although intuitively, the sech$+$ and sech$-$ pulses should interact with Rb vapor in similar ways, they do not when the OD of the Rb is high and the laser pulses are intense. This pump-probe experiment gives a lifetime of about 8 ps for the feature, which is much longer than the collisional lifetime of 1.7 ps.

In conclusion, in these experiments we have observed coherent effects that arise when shaped ultrafast laser pulses propagate through an optically dense medium. These effects include pulse reshaping, self-focusing, and stimulated emission. We have shown that the pulse shaper can be used to control the nature of the pulse reshaping in atomic rubidium. Furthermore, we have characterized both the spectral and temporal aspects of this reshaping using the STRUT. We have found, both theoretically and experimentally, that the three pulse shapes of our experiments excite the atomic system in different fashions. Gain in pulses propagating through the Rb system is evident in our pump-probe studies, and this gain is observed to persist on a time scale longer than the collisional lifetime T_2. We observe that the sech$-$ pulse is the most efficient among the three pulse shapes at generating this gain. This demonstrates the capability of the pulse shaping system in controlling the dynamics of the excited state atoms. This work may have applications in the excitation of rubidium for the production of spin-polarized noble gases.

We gratefully acknowledge the contributions of Mike Souza, Rahim Rizi, and Dorine Keusters.

[1] C. J. Bardeen, Q. Wang, and C. V. Shank, J. Phys. Chem. A **102**, 2759 (1998); C. J. Bardeen *et al.*, J. Phys. Chem. A **101**, 3815 (1997); W. S. Warren, H. Rabitz, and M. Dahleh, Science **259**, 1581 (1993); J. S. Melinger *et al.*, J. Chem. Phys. **101**, 6439 (1994).

[2] S. A. Diddiams *et al.*, Opt. Photonics News **9**, 37 (1998); T. C. Weinacht, J. Ahn, and P. H. Bucksbaum, Phys. Rev. Lett. **81**, 3050 (1998).

[3] W. S. Warren, Science **242**, 848 (1988); W. S. Warren and M. Silver, Adv. Magn. Reson. **12**, 248 (1988); A. Assion *et al.*, Science **282**, 919 (1998).

[4] J. X. Tull, M. A. Dugan, and W. S. Warren, Adv. Magn. Opt. Reson. **20**, 1 (1997); A. M. Weiner, Prog. Quantum Electron. **19**, 161 (1995).

[5] M. S. Silver, R. I. Joseph, C. N. Chen, V. J. Sank, and D. I. Hoult, Nature (London) **310**, 681 (1984); F. T. Hioe, Phys. Rev. A **30**, 2100 (1984).

[6] T. G. Walker and W. Happer, Rev. Mod. Phys. **69**, 629 (1997).

[7] L. Allen and J. Eberly, *Optical Resonance and Two-Level Atoms* (Dover, New York, 1987).

[8] F. Spano and W. S. Warren, Phys. Rev. A **37**, 1013 (1988).

[9] S. T. Hendow and S. A. Shakir, Appl. Opt. **25**, 1759 (1986).

[10] D. Rosenfeld and Y. Zur, J. Magn. Reson. **132**, 102 (1998).

[11] J. K. Ranka *et al.*, Phys. Rev. A **57**, R36 (1998).

[12] M. R. Fetterman *et al.*, Opt. Exp. **310**, 366 (1998).

[13] J.-K. Rhee *et al.*, J. Opt. Soc. Am. B **13**, 1780 (1996).

[14] D. N. Fittinghoff, J. L. Bowie, J. N. Sweetser, R. T. Jennings, M. A. Krumbugel, K. W. DeLong, and R. Trebino, Opt. Lett. **21**, 1313 (1996).

[15] C. Iaconis and I. A. Walmsley, Opt. Lett. **23**, 792 (1998).

[16] A. A. Radzig and B. M. Smirnov, *Reference Data on Atoms, Molecules, and Ions* (Springer-Verlag, New York, 1985).